Electronic Supplementary Information for Robust Folding of Elastic Origami

M. E. Lee-Trimble,*[a] Ji-Hwan Kang,[b,c] Ryan C. Hayward,[b,d] and Christian D. Santangelo[a,e]

I. ELASTIC MODULI OF TRILAYER ORIGAMI

Our estimates of elastic moduli will be based on the estimates $Y_N/Y_p \sim 5 \times 10^{-4}$ and $h_p/h_N \sim 0.04$.

A. Estimate of the stretching energy of elastic origami

We estimate the elastic energy of a face according to

$$E = \frac{1}{2}\int dA \left[\int_{-h_N/2-h_P}^{-h_N/2} dz\ Y_p + \int_{-h_N/2}^{h_N/2} dz\ Y_N + \int_{h_N/2}^{h_N/2+h_P} dz\ Y_p\right]\gamma^2, \tag{1}$$

where Y_N and Y_p are the three dimensional Young's moduli and h_N is the thickness of the hydrogel layer, h_P is the thickness of each polymer layer, and γ is a dimensionless strain.

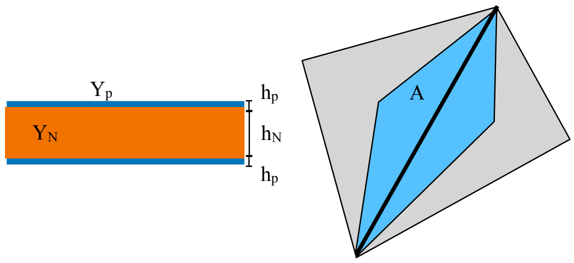

FIG. 1: (left) a cross-section of a trilayer origami face showing the thicknesses and three-dimensional Young's moduli. (right) the area of each face adjacent to an edge that is closer to that edge than any other.

Then assuming that γ is approximately constant across a face and assuming $Y_p h_P \gg Y_N h_N$, we obtain

$$E \approx Y_p h_p A \gamma^2. \tag{2}$$

For the area, A and an edge surrounded by two faces, we use the area in Fig. 1, which is conveniently one third the total area of the two adjoining faces. For edges on the boundary, the corresponding stretching energy is obtained from a single face. Comparing this to our spring energy,

$$E = \frac{1}{2}\kappa_S \gamma^2, \tag{3}$$

we obtain an estimate $\kappa_{S,I} \approx 2Y_p h_p A_I$ for the stretching modulus associated with edge I, where A_I is the appropriately chosen area.

[a] *Department of Physics, University of Massachusetts Amherst, Amherst, MA, 01003*
[b] *Department of Polymer Science and Engineering, University of Massachusetts Amherst, Amherst, MA, 01003*
[c] *Department of Chemical Engineering, California State University Long Beach, Long Beach, CA, 90840*
[d] *Department of Chemical and Biological Engineering, University of Colorado Boulder, Boulder, CO, 80309. E-mail: ryan.hayward@colorado.edu*
[e] *Department of Physics, Syracuse University, Syracuse, NY, 13244. E-mail: cdsantan@syr.edu*

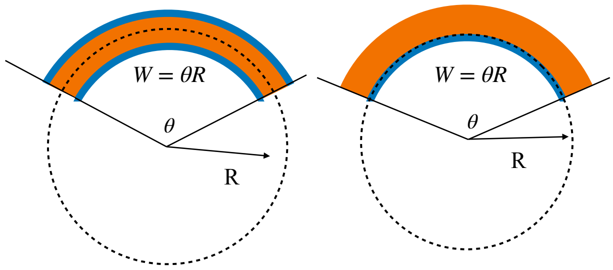

FIG. 2: Bending a face or a fold to have constant curvature R^{-1}. The angle θ is identical to the apparent fold angle of the fold. When bending a face (left), we assume the face bends along the midsurface whereas for an active fold, we assume the surface bends along the stiffest layer.

B. The bending modulus of the folds

For an active fold, we assume the fold is bent along a width W_I to a constant curvature R, so that $R = W_I/\theta$. Therefore, the bending energy of a face can be approximately computed as

$$\begin{aligned} E_B &= \frac{1}{2}\frac{Y_N}{1-\nu^2}WL\int_{-h_N/2}^{h_N/2} dz\frac{z^2}{R^2} + \frac{1}{2}\frac{Y_p}{1-\nu^2}WL\int_{-h_N/2-h_P}^{-h_N/2} dz\frac{z^2}{R^2} + \frac{1}{2}\frac{Y_p}{1-\nu^2}WL\int_{h_N/2}^{h_N/2+h_P} dz\frac{z^2}{R^2} \quad (4)\\ &\approx \frac{1}{2}\theta^2 L\frac{Y_p h_N^2 h_P}{2W(1-\nu^2)} \quad (5)\end{aligned}$$

Thus, $\kappa_{face,I} \approx L_I/W_I(Y_p h_N^2 h_P)/(2(1-\nu^2))$. For an active fold we obtain

$$\begin{aligned} E_B &= \frac{1}{2}\frac{Y_N}{1-\nu^2}WL\int_{h_P/2}^{h_N+h_P/2} dz\frac{z^2}{R^2} + \frac{1}{2}\frac{Y_p}{1-\nu^2}WL\int_{-h_P/2}^{h_p/2} dz\frac{z^2}{R^2} \quad (6)\\ &\approx \frac{1}{2}\theta^2 L\frac{Y_N h_N^3}{3W(1-\nu^2)} \quad (7)\end{aligned}$$

Thus, $\kappa_{fold,I} \approx L_I/W_I Y_N h_N^3/(3(1-\nu^2))$. We expect that the width of an active fold is set by the size of the cut used to create the folding face whereas the width of a fold associated with bending a face is set by the size of a vertex which is also the width of the trenches. Therefore, we assume W_I is the same for both types of folds.

C. Stiffness ratios

In our numerical calculations, we divide all the moduli by $2Y_p h_p A$ where A is the characteristic area. Neglecting the Poisson ratio, we use

$$\begin{aligned} \kappa_{S,I} &\approx A_I/A \\ \kappa_{fold,I} &\approx \frac{L_I}{\ell}\left(\frac{Y_N}{Y_p}\frac{\ell}{W}\frac{h_N^3}{6h_p A}\right) \\ \kappa_{face,I} &\approx \frac{L_I}{\ell}\left(\frac{h_N^2\ell}{4WA}\right)\end{aligned} \quad (8)$$

where ℓ is the characteristic length of a fold. For $h_P \approx 0.2\mu m$, $h_N \approx 5\mu m$, $Y_N/Y_p \approx 5\times10^{-4}$, $W \approx 44\mu m$, $A \approx 2\times10^4\mu m^2$, and $\ell \approx 260\mu m$, we obtain $\kappa_{fold,I} \approx 2\times10^{-5}L_I/\ell$ and $\kappa_{face,I} \approx 2\times10^{-3}L_I/\ell$, or $K_{fold} = 2\times10^{-5}$ and $K_{face} = 2\times10^{-3}$

II. ENERGY OF NEARLY FLAT ORIGAMI

To derive the elastic energy for nearly flat origami in the small strain limit, we assume we have already added face folds so that the origami is built from only triangular faces. We then define a vector function of the vertex positions

$$f_i(\mathbf{u}) = \frac{\sqrt{K_i}}{2}\left(\frac{L_i^2}{\bar{L}_i^2} - 1\right) \tag{9}$$

where $\mathbf{u} = (\mathbf{X}_1, \cdots \mathbf{X}_V)$ is a vector containing the position of all V vertices. Then the stretching energy is written as

$$E_S = \frac{1}{2}\sum_{i=1}^{E} f_i(\mathbf{u})^2. \tag{10}$$

We now expand $f_i(\mathbf{u})$ around the flat state $\mathbf{u}_0$ to find

$$f_i(\mathbf{u}_0 + \delta\mathbf{u}) \approx \partial_n f_i(\mathbf{u}_0)\delta u^n + \frac{1}{2}\partial_n\partial_m f_i(\mathbf{u}_0)\delta u^n \delta u^m \tag{11}$$

We next construct an orthonormal basis in the space of possible edges indexed by i, $\{\sigma_{1,i}, \cdots, \sigma_{S,i}, e_{1,i}, \cdots, e_{E-S,i}\}$ where $\sum_i \sigma_{N,i}\partial_n f_i(\mathbf{u}_0) = 0$. The $\sigma_{N,i}$ are, therefore, the components of the self-stresses of the linkage representing the origami structure.

Now the energy can be written as

$$\begin{aligned} E_S &= \frac{1}{2}\sum_{N=1}^{E-S}\left[\sum_i e_{N,i}\left(\partial_n f_i(\mathbf{u}_0)\delta u^n + \frac{1}{2}\partial_n\partial_m f_i(\mathbf{u}_0)\delta u^n\delta u^m\right)\right]^2 \\ &\quad + \frac{1}{2}\sum_{N=1}^{S}\left(\sum_i \sigma_{N,i}\frac{1}{2}\partial_n\partial_m f_i(\mathbf{u}_0)\delta u^n\delta u^m\right)^2 \end{aligned} \tag{12}$$

Finally, we drop higher order contributions to the first term to obtain

$$E_S = \frac{1}{2}\sum_{N=1}^{E-S}\left(\sum_i e_{N,i}\partial_n f_i(\mathbf{u}_0)\delta u^n\right)^2 + \frac{1}{8}\sum_{N=1}^{S}\left(\sum_i \sigma_{N,i}\partial_n\partial_m f_i(\mathbf{u}_0)\delta u^n\delta u^m\right)^2. \tag{13}$$

The first term is the harmonic contribution to the energy. For flat origami, we know that these correspond to the in-plane motions. On the other hand, the second term corresponds to the out-of-plane motion of the vertices. Finally, we note that the number of self-stresses S is given by the number of internal vertices V_I.

For small strains, we assume that the first term is zero so that only out-of-plane deformations can occur. Finally, we obtain an approximate energy for flat origami near the flat state as a sum of terms quartic in the vertical displacements of the vertices,

$$E_S \approx \frac{1}{8}\sum_{N=1}^{V_I}\left(\sum_{n=1}^{V}\sum_{m=1}^{V} Q_{Nnm}h_n h_m\right)^2, \tag{14}$$

where h_n is the height of the n^{th} vertex above the xy-plane and

$$Q_{Nnm} = \sum_i \sqrt{K_{S,i}}\sigma_{N,i}\left.\frac{\partial}{\partial h_n}\frac{\partial}{\partial h_m}\gamma_i\right|_{h_n=0}, \tag{15}$$

where γ_i is the strain of the i^{th} edge defined in the main text.

III. ALTERNATE MODEL WITH ELASTIC POLYGON FACES

The in-plane elastic energy for a Hookean, isotropic two-dimensional solid can be written as

$$E_{el} = \frac{1}{2}\lambda\left(\sum_i \gamma_{ii}\right)^2 + \mu\sum_{ij}\gamma_{ij}^2, \tag{16}$$

where $\gamma_{ij} = \partial_i u_j + \partial_j u_i$ and λ and μ are the Lamè coefficients. We assume that each triangular face has an energy of the form of Eq. (16). The in-plane elastic deformations u_i are determined by assuming the face has deformed affinely. For a triangular face on the $xy-$plane, this uniquely determines the displacement and allows us to estimate the elastic energy of arbitrarily deformed triangular faces.

To compare this to our linear spring edge model, we use the same method for plotting the phase diagrams for the birdsfoot as in the main body of the paper but with the above energy. Fig. 3 shows a side-by-side comparison of the resulting plots generated by the two different energies at the experimental values for default and softened faces. Minimizing the more complicated elastic polygon energy is more computationally costly, so the grid size has been reduced and grid squares with black lines denote points that failed to converge, with their color assigned based on neighboring squares. The agreement between models overall is good, even without fitting parameters.

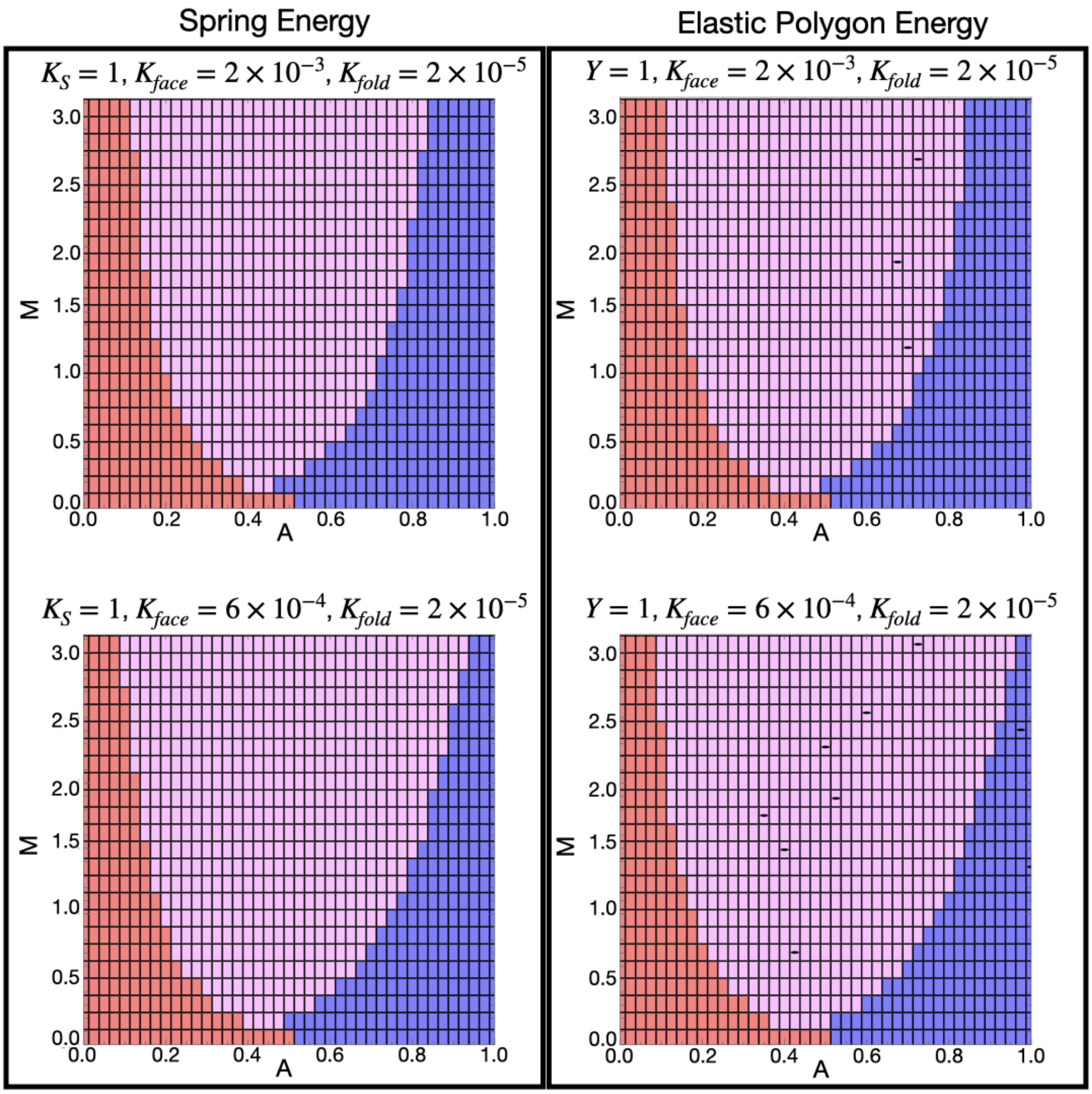

FIG. 3: Phase diagrams for the birdsfoot with axes of the magnitude of the target angles, M, and the control parameter A, as described in the main body of the paper. The blue and red regions represent only one branch appearing while the center pink region represents the bistable region. The left column uses the linear spring edge model for face stretching while the right column uses the elastic polygon model. The top row has torsion spring constants corresponding to experiment with default faces while the bottom row corresponds to softened faces.

IV. PROGRAMMED TARGET ANGLES FOR THE RANDLETT BIRD SIMULATIONS

We use the same programmed fold angles for both the experiment and the simulations. They can be seen in Fig. 4.

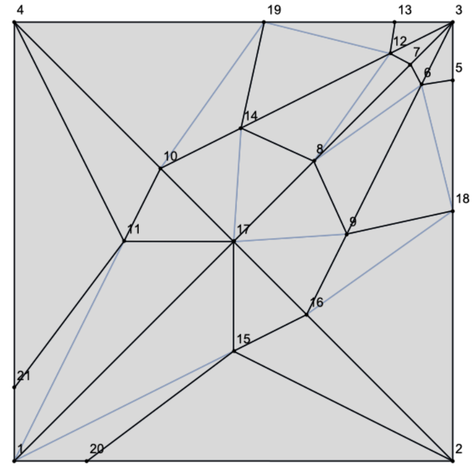

Fold (by vertices)	Programmed Fold Angle
{1, 11}	0
{1, 15}	0
{1, 17}	$-79\pi/180$
{2, 15}	$143\pi/180$
{3, 6}	$139\pi/180$
{3, 7}	$-107\pi/180$
{3, 12}	$139\pi/180$
{4, 10}	$-13\pi/15$
{4, 11}	$143\pi/180$
{5, 6}	$-149\pi/180$
{6, 7}	$-149\pi/180$
{6, 8}	0
{6,18}	0
{7, 12}	$-149\pi/180$
{8, 7}	$107\pi/180$
{8, 12}	0
{8, 14}	$34\pi/45$
{8, 17}	$-91\pi/180$
{9, 6}	$-23\pi/30$
{9, 8}	$34\pi/45$

Fold (by vertices)	Programmed Fold Angle
{9, 17}	0
{9, 18}	π
{10, 11}	$-17\pi/30$
{10, 17}	$-13\pi/15$
{10, 19}	0
{11, 21}	$41\pi/60$
{12, 13}	$-149\pi/180$
{12, 19}	0
{14,10}	$157\pi/180$
{14, 12}	$-23\pi/30$
{14, 17}	0
{15, 16}	$-17\pi/30$
{15, 17}	$43\pi/60$
{16, 2}	$-13\pi/15$
{16, 9}	$157\pi/180$
{16, 18}	0
{17, 11}	$43\pi/60$
{17, 16}	$-13\pi/15$
{19, 14}	π
{20,15}	$41\pi/60$

FIG. 4: (left) the Randlett bird with true folds in black and added face folds in lighter blue with vertices numbered. (right) the programmed fold angles used in the simulations. Folds are denoted by their end vertices.